

Breathers and surface modes in oscillator chains with Hertzian interactions

Guillaume James^{**}, Jesús Cuevas[†] and Panayotis G. Kevrekidis[‡]

* Laboratoire Jean Kuntzmann, Université de Grenoble and CNRS
BP 53, 38041 Grenoble Cedex 9, France

* INRIA, Bipop Team-Project

ZIRST Montbonnot, 655 Avenue de l'Europe, 38334 Saint Ismier, France

†Grupo de Física No Lineal, Departamento de Física Aplicada I, Escuela Politécnica Superior, Universidad de Sevilla
C/ Virgen de África, 7, 41011 Sevilla, Spain

‡Department of Mathematics and Statistics, University of Massachusetts
Amherst, Massachusetts 01003-4515, USA

Email: guillaume.james@imag.fr, jcuevas@us.es, kevrekid@math.umass.edu

Abstract—We study localized waves in chains of oscillators coupled by Hertzian interactions and trapped in local potentials. This problem is originally motivated by Newton's cradle, a mechanical system consisting of a chain of touching beads subject to gravity and attached to inelastic strings. We consider an unusual setting with local oscillations and collisions acting on similar time scales, a situation corresponding e.g. to a modified Newton's cradle with beads mounted on stiff cantilevers. Such systems support static and traveling breathers with unusual properties, including double exponential spatial decay, almost vanishing Peierls-Nabarro barrier and spontaneous direction-reversing motion. We prove analytically the existence of surface modes and static breathers for anharmonic on-site potentials and weak Hertzian interactions.

Granular media are known to display a rich dynamical behavior originating from their complex spatial structure and different sources of nonlinearity (Hertzian contact interactions between grains, friction, plasticity). In the case of granular crystals (i.e. for grains organized on a lattice), nonlinear contact interactions lead to different types of localized wave phenomena that could be potentially used for the design of smart materials such as acoustic diodes [1]. Among the most studied types of excitations, solitary waves can be easily generated by an impact at one end of a chain of touching beads (see [7, 8] and references therein). In the absence of an original compression in the chain (the so-called precompression), these solitary waves differ from the classical KdV-type solitary waves, since they are highly-localized (with super-exponential decay) and their width remains unchanged with amplitude (see e.g. [12]). These properties originate from the fully nonlinear character of the Hertzian interaction potential $V(r) = \frac{2}{5} \gamma (-r)_+^{5/2}$ (with $\gamma > 0$ and $(a)_+ = \max(a, 0)$), which yields a vanishing sound velocity in the absence of precompression.

Discrete breathers (i.e. intrinsic localized modes) form another interesting class of excitations consisting of time-periodic and spatially localized waveforms [6, 3]. These

waves exist in diatomic granular chains under precompression [2, 13] (with their frequency lying between the acoustic and optic phonon bands) and can be generated e.g. through modulational instabilities. However, because precompression suppresses the fully nonlinear character of Hertzian interactions, these excitations inherit the usual properties of discrete breathers, i.e. their spatial decay is exponential and their width diverges at vanishing amplitude (for frequencies close to the bottom of the optic band).

The situation is sensibly different for granular systems without precompression. In that case, localized oscillations can be generated on short transients in the form of transitory defect modes induced by a mass impurity (see [11] and references therein) but never occur *time-periodically* as proved in [5]. Indeed, uncompressed granular chains are described by the Fermi-Pasta-Ulam lattice with Hertzian interactions

$$\ddot{y}_n = V'(y_{n+1} - y_n) - V'(y_n - y_{n-1}) \quad (1)$$

(or spatially inhomogeneous variants thereof), where $y_n(t)$ denotes the n th bead displacement from its reference position. For all T -periodic solutions of (1), the average interaction forces $\int_0^T V'(y_{n+1} - y_n) dt$ are independent of n (this is immediate by integrating (1)). Consequently, localized oscillations would yield a vanishing average interaction force between grains, which is impossible since Hertzian interactions are repulsive under contact and vanish otherwise.

In contrast to the above picture, we have numerically established in [5] the existence of time-periodic localized oscillations in Hertzian chains with symmetric local potentials described by the system

$$\ddot{y}_n + W'(y_n) = V'(y_{n+1} - y_n) - V'(y_n - y_{n-1}) \quad (2)$$

where $W(y) = \frac{1}{2} y^2 + \frac{s}{4} y^4$ and $s \in \mathbb{R}$ measures the local anharmonicity. System (2) describes small amplitude waves in a Newton's cradle [4] (figure 1, left) or other mechanical systems consisting of beads mounted e.g. on an elastic matrix [10] or cantilevers [5] (figure 1, right). In the last two

cases, local oscillations and collisions between beads can occur on similar time scales for realistic material parameter values, which allows for breathing dynamics to take place. Static and moving breathers can be generated from standard initial conditions such as a localized impact [5, 10] or perturbations of unstable periodic traveling waves [4].

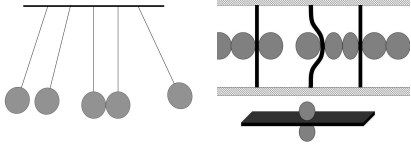


Figure 1: Left : prototypical Newton's cradle consisting of a chain of beads attached to pendula. Right : array of clamped cantilevers decorated by spherical beads.

Let us summarize the results of [5]. Two families of static breather solutions of (2) (parametrized by their frequency $\omega_b > 1$) have been computed using the Gauss-Newton method and path-following. The first one consists of bond-centered breathers satisfying $y_n(t) = -y_{-n+1}(t) := \mathcal{S}_1 y_n(t)$, and the second corresponds to site-centered breathers with $y_n(t) = -y_{-n}(t + T_b/2) := \mathcal{S}_2 y_n(t)$, where T_b denotes the breather period (each solution family is invariant by a symmetry \mathcal{S}_i of (2)). Profiles of both breather types are given in figure 2 for a particular frequency close to unity (i.e. the linear frequency of local oscillators), a limit where the breather amplitude vanishes. Near this limit, quasi-continuum approximations of the breather profiles can be derived [5], namely

$$y_n^{(1)}(t) = 2\epsilon(-1)^n [g(n) + g(n-1)] \cos(\omega_b t) \quad (3)$$

for bond-centered breathers and

$$y_n^{(2)}(t) = 2\epsilon(-1)^n [g(n + \frac{1}{2}) + g(n - \frac{1}{2})] \cos(\omega_b t) \quad (4)$$

for site-centered ones, where $\omega_b = 1 + \frac{\epsilon^{1/2}}{2\tau_0}$ ($\tau_0 \approx 1.545$), $g(x) = (\frac{3}{10})^3 \cos^6(\frac{x}{3})$ for $|x| \leq \frac{3\pi}{2}$ and $g = 0$ elsewhere. Figure 2 compares the numerical solutions with the above approximations for $\omega_b \approx 1$, showing excellent agreement. Obviously discrepancies appear at larger amplitude, since approximations (3) and (4) retain only one Fourier mode and are independent of the local anharmonicity (which is dominated by the Hertzian nonlinearity at small amplitude). The above approximations possess compact supports (with a width independent of ω_b), but the breathers computed numerically do not share this property strictly speaking and instead display super-exponential localization (this is in analogy with the case of homogeneous polynomial interaction potentials, see section 4.1.3 of [3]).

Dynamical simulations of [5] indicate that extremely small perturbations of the static breathers can lead to their translational motion (generating a so-called traveling

breather), for anharmonic on-site potentials, but more critically even in the harmonic case. This phenomenon is linked with an extremely small difference between the energies \mathcal{H} of site- and bond-centered breathers having the same frequency (the so-called approximate Peierls-Nabarro barrier). Typical values of breather energies are given in figure 3, where $\mathcal{H} = \sum_n e_n$ and $e_n = \frac{1}{2} \dot{y}_n^2 + W(y_n) + V(y_{n+1} - y_n)$. Another manifestation of the high breather mobility is the systematic formation of a travelling breather after an impact at one end of the oscillator chain (see figure 4).

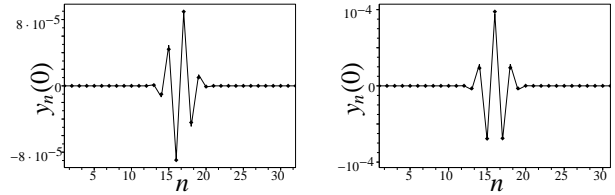


Figure 2: Bond-centered (left plot) and site-centered (right plot) breather solutions of (2) for $\omega_b = 1.01$ (potential parameters are $\gamma = 1$ and $s = 0$). The numerical solutions (marks) are compared to the quasi-continuum approximations $y_n^{(1)}$, $y_n^{(2)}$ (continuous lines).

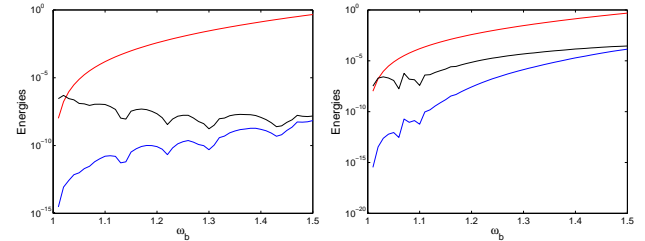


Figure 3: Breather energies versus frequency ω_b , when the on-site potential is harmonic ($s = 0$, left plot) or anharmonic ($s = -1/6$, right plot) and $\gamma = 1$. The red curves give the energy \mathcal{H}_{bc} of bond-centered breathers, the blue curves the approximate Peierls-Nabarro barrier E_{PN} (energy difference between site- and bond-centered breathers) and the black curves the relative energy ratio E_{PN}/\mathcal{H}_{bc} . For small amplitude breathers (i.e. $\omega_b \approx 1$), the different values of s yield comparable values of E_{PN} . Clearly E_{PN} increases with breather amplitude but remains very small in this parameter range (e.g. E_{PN} is close to 10^{-4} for $\omega_b = 1.5$ and $s = -1/6$). The harmonic case yields even smaller barriers, by 3 – 4 orders of magnitude for $\omega_b = 1.3$.

Different phenomena have been identified in [5] depending on the softening or hardening character of the local potential W . Firstly, the stability of both site-centered and bond-centered breathers is critically dependent on the strength (and sign) of the anharmonicity (we refer to [5] for more details). Secondly, depending whether $s < 0$ or $s > 0$,

the occurrence of surface mode excitations (i.e. oscillations localized near a boundary) or direction-reversing traveling breathers was observed after an impact. Both phenomena are illustrated by figures 4 and 5. The origin of direction reversal is still unclear at the present stage, although we think it might originate from the interaction between the traveling breather and nonlinear waves confined between the breather and the boundary (figure 5, right plot).

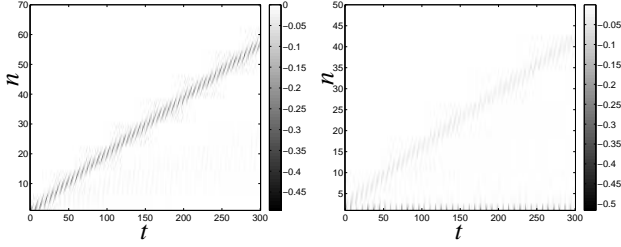


Figure 4: Space-time diagrams showing the interaction forces $f_n = -(y_n - y_{n+1})_+^{3/2}$ in system (2) with $\gamma = 1$ and free end boundary conditions. Forces are represented in grey levels, white corresponding to vanishing interactions (beads not in contact) and black to a minimal negative value of the contact force. The initial condition is $y_n(0) = 0$ for $n \geq 1$, $\dot{y}_n(0) = 0$ for $n \geq 2$, $\dot{y}_1(0) = 0.94$. For an harmonic local potential ($s = 0$, left plot), a traveling breather is generated. For a soft local potential ($s = -0.7$, right plot), one observes in addition the excitation of a surface mode.

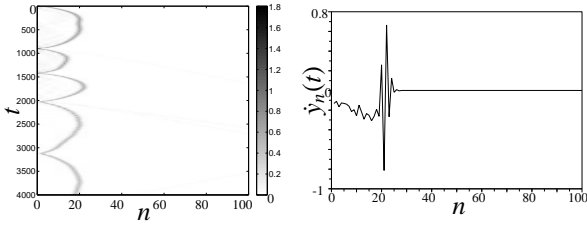


Figure 5: Left : space-time diagram of the energy density e_n for system (2) with $\gamma = 1$ and a hard anharmonic local potential ($s = 1$). The initial condition is the same as in figure 4 except $\dot{y}_1(0) = 1.9$. Right : corresponding particle velocities close to direction-reversing ($t \approx 241$).

In order to understand the absence of surface mode excitation observed in figure 5 for $s = 1$, we now analyze the properties of surface modes computed by the Gauss-Newton method (all numerical computations are performed for $\gamma = 1$). The results are shown in figure 6 (left column). For $s = 1$, surface modes exist for frequencies ω_s lying above a critical frequency $\omega_{\min} \approx 1.96$, where a pair of Floquet eigenvalues converges towards unity (spectra not shown here). For $\omega_s \approx \omega_{\min}$ these solutions are spectrally stable and one can observe an energy threshold. This explains why a surface mode is not observed in figure 5 where

the energy of the initial excitation is well below the excitation threshold. This situation contrasts with the case of soft local potentials illustrated in figure 6 (right column). For $s = -0.7$, surface modes exist for $\omega_s \in [0.705, 1)$. They are spectrally stable for $\omega_s \approx 1$ but oscillatory instabilities appear at smaller frequencies (spectra not shown here). When $\omega_s \rightarrow 1$, their energy and amplitude vanish, opening the possibility of exciting such modes for arbitrarily small initial velocities of the first particle.

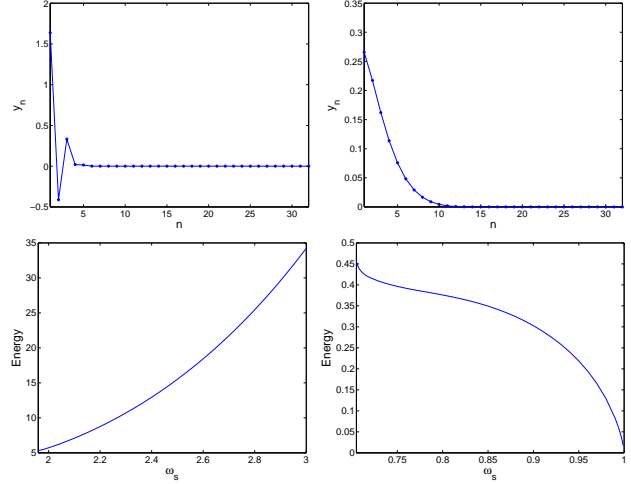


Figure 6: Top : profile of a surface mode at the instant of maximal amplitude, for a hard local potential ($s = 1$, $\omega_s = 2$, left plot) and a soft one ($s = -0.7$, $\omega_s = 0.99$, right plot). Bottom : energy of the surface mode versus frequency ω_s , for $s = 1$ (left plot) and $s = -0.7$ (right plot).

Having numerically analyzed the properties of surface modes of (2) when γ (the stiffness constant of Hertzian interactions) equals unity, we now prove the existence of time-periodic and spatially localized solutions when γ is small. The small coupling (anticontinuum) limit was introduced in reference [6] (and considerably generalized in [9]) and applies both to breathers and surface modes. From a physical point of view, this parameter regime can be realized with an array of clamped cantilevers (see figure 1) decorated by spherical beads made from a sufficiently soft material (e.g. rubber). In addition, the anticontinuum limit requires an anharmonic local potential W , i.e. $s \neq 0$.

We consider system (2) for $n \in \Gamma$, with $\Gamma = \mathbb{Z}$ for discrete breathers (case of a doubly infinite chain) and $\Gamma = \mathbb{N}_0$ for surface modes (semi-infinite chain, with free-end boundary conditions at $n = 0$). For $\gamma = 0$, system (2) admits localized periodic solutions satisfying $y_n = 0 \forall n \neq 0$, $\ddot{y}_0 + W'(y_0) = 0$ and $y_0(t + T_0) = y_0(t)$. Setting $\dot{y}_0(0) = 0$, $a := y_0(0) > 0$ and $T_0 \equiv T_0(a)$, it is a classical result that $s T_0'(a) < 0$. Consequently, the time periodic oscillations y_0 can be parametrized by their period T_0 , with $T_0 < 2\pi$ for $s > 0$ and $T_0 > 2\pi$ for $s < 0$. We shall denote by $Y_{0, T_0} := (y_n)_n$ the even T_0 -periodic solution constructed

above for $\gamma = 0$. Now let us assume $T_0 \notin 2\pi\mathbb{N}$ (this condition is automatically satisfied for $s > 0$). Thanks to this nonresonance condition, one can apply the persistence theorem for normally non-degenerate discrete breathers proved in reference [9] (section 3.5), which readily applies to system (2) since $V \in C^2(\mathbb{R})$ has sufficient smoothness. More precisely, for γ small enough in system (2), this result ensures the existence of a family of localized solutions $Y_{\gamma,T}(\cdot + \phi)$ parametrized by their period $T \approx T_0$ (since $T'_0 \neq 0$) and an arbitrary phase ϕ . In addition the perturbed and unperturbed solutions are close when γ is small, i.e. one has $Y_{\gamma,T} = Y_{0,T} + O(\gamma)$ in $C^2(S^1; \ell_2(\Gamma))$ (we denote $S^1 = \mathbb{R}/(T\mathbb{Z})$). Note that the corresponding breather solutions are site-centered, due to the local uniqueness of $\gamma \mapsto Y_{\gamma,T}$ and the invariance of (2) by the symmetry \mathcal{S}_2 . Similarly, starting from a bond-centered breather for $\gamma = 0$ (with $y_1 = -y_0$, $y_n = 0$ elsewhere) allows one to obtain bond-centered breathers for $\gamma \approx 0$. More generally, multi-breathers having many excited sites can be constructed in the same way at small coupling.

Now let us estimate the spatial decay of breathers and surface modes. Consider a T -periodic solution of (2) satisfying the nonresonance condition $T \notin 2\pi\mathbb{N}$. We assume this solution is spatially localized, i.e. its supremum norm $v_n = \|y_n\|_\infty := \sup_{t \in [0, T]} |y_n(t)|$ satisfies $\lim_{|n| \rightarrow +\infty} v_n = 0$. In order to estimate v_n , we rewrite (2) in the form

$$y_n = L^{-1} \left(\gamma (y_{n-1} - y_n)_+^{3/2} - \gamma (y_n - y_{n+1})_+^{3/2} - s y_n^3 \right), \quad (5)$$

where $L = \partial_t^2 + I : C^2(S^1; \mathbb{R}) \rightarrow C^0(S^1; \mathbb{R})$ is invertible thanks to the nonresonance assumption. By using (5), there exists $C > 0$ and $m \in \mathbb{N}_0$ such that for $|n| \geq m + 1$ we have $v_n \leq \frac{C}{3} (v_{n+1}^{3/2} + v_n^{3/2} + v_{n-1}^{3/2})$. Introducing the sequence $\epsilon_j = \sup_{|k| \geq j} v_k$, it follows that $\epsilon_j \leq C \epsilon_{j-1}^{3/2}$ for $j \geq m + 1$, hence one obtains by induction

$$\epsilon_j \leq C^{-2} \lambda^{(3/2)^j}, \quad \lambda = (C^2 \epsilon_m)^{(2/3)^m}, \quad j \geq m. \quad (6)$$

Since $\lim_{j \rightarrow +\infty} \epsilon_j = 0$, we can fix m such that $\lambda < 1$. Estimate (6) implies $\|y_n\|_\infty \leq \epsilon_{|n|} \leq C^{-2} \lambda^{(3/2)^{|n|}}$ for $|n| \geq m$, i.e. the solution decays doubly exponentially at infinity.

As a conclusion, we have reviewed recent results of [5] on the numerical observation of breathers and surface modes in granular chains with stiff local potentials. We have found the existence of an energy threshold for hard surface modes, which explains their non-excitation by moderate impacts reported in [5]. We have obtained doubly exponential decay estimates for breathers and surface modes and proved their existence for anharmonic local potentials when $\gamma \approx 0$. The persistence of these solutions for larger values of γ is numerically observed (for $\gamma = 1$) but remains an open question from an analytical point of view. In addition, the spontaneous direction-reversing motion of discrete breathers occurring for hard local potentials and the smallness of their Peierls-Nabarro energy barrier has yet to be understood.

Acknowledgments

J.C. acknowledges support from the MICINN project FIS2008-04848 & P.G.K. from the NSF (grant CMMI-1000337), from the A.S. Onassis Public Benefit Foundation (grant RZG 003/2010-2011) and from AFOSR (grant FA9550-12-1-0332).

References

- [1] N. Boechler, G. Theocharis and C. Daraio. Bifurcation-based acoustic switching and rectification, *Nat. Mater.* 10 (2011), 665-668.
- [2] N. Boechler, G. Theocharis, S. Job, P.G. Kevrekidis, M.A. Porter and C. Daraio. Discrete breathers in one-dimensional diatomic granular crystals, *Phys. Rev. Lett.* 104 (2010), 244302.
- [3] S. Flach and A. Gorbach. Discrete breathers : advances in theory and applications, *Phys. Rep.* 467 (2008), 1-116.
- [4] G. James. Nonlinear waves in Newton's cradle and the discrete p -Schrödinger equation, *Math. Models Meth. Appl. Sci.* 21 (2011), 2335-2377.
- [5] G. James, P.G. Kevrekidis and J.Cuevas. Breathers in oscillator chains with Hertzian interactions (2011), arXiv:1111.1857v1 [nlin.PS]. Submitted to *Physica D*.
- [6] R.S. MacKay and S. Aubry. Proof of existence of breathers for time-reversible or Hamiltonian networks of weakly coupled oscillators, *Nonlinearity* 7 (1994), 1623-1643.
- [7] V.F. Nesterenko, *Dynamics of heterogeneous materials*, Springer Verlag, 2001.
- [8] N.-S. Nguyen and B. Brogliato. Shock dynamics in granular chains: numerical simulations and comparison with experimental tests, *Granular Matter* 14 (2012), 341-362.
- [9] J.-A. Sepulchre and R.S. MacKay. Localized oscillations in conservative or dissipative networks of weakly coupled autonomous oscillators, *Nonlinearity* 10 (1997), 679-713.
- [10] Y. Starosvetsky, M. Arif Hasan, A.F. Vakakis and L.I. Manevitch. Strongly nonlinear beat phenomena and energy exchanges in weakly coupled granular chains on elastic foundations, *SIAM J. Appl. Math.* 72 (2012), 337-361.
- [11] Y. Starosvetsky, K. R. Jayaprakash and A.F. Vakakis. Scattering of solitary waves and excitation of transient breathers in granular media by light intruders, *J. Appl. Mech.* 79 (2012), 011001.
- [12] A. Stefanov and P.G. Kevrekidis. On the existence of solitary traveling waves for generalized Hertzian chains, *J. Nonlinear Sci.* 22 (2012), 327-349.
- [13] G. Theocharis, N. Boechler, P. G. Kevrekidis, S. Job, M.A. Porter, and C. Daraio. Intrinsic energy localization through discrete gap breathers in one-dimensional diatomic granular crystals, *Phys. Rev. E.* 82 (2010), 056604.